Pectin Methyl Esterase Inhibits Intrusive and Symplastic Cell Growth in Developing Wood Cells of *Populus*[1,2][W][OA]

Anna Siedlecka, Susanne Wiklund, Marie-Amélie Péronne, Fabienne Micheli[3], Joanna Leśniewska[4], Ingmar Sethson, Ulf Edlund, Luc Richard, Björn Sundberg*, and Ewa J. Mellerowicz

Department of Forest Genetics and Plant Physiology, Umeå Plant Science Centre, SE 901 83 Umeå, Sweden (A.S., M.-A.P., J.L., B.S., E.J.M.); Organic Chemistry, Umeå University, SE 901 87 Umeå, Sweden (S.W., I.S., U.E.); and Laboratoire de Physiologie Cellulaire et Moléculaire des Plantes, Université Pierre et Marie Curie, CNRS-FRE 2846, F94200 Ivry sur Seine, France (F.M., L.R.)

Wood cells, unlike most other cells in plants, grow by a unique combination of intrusive and symplastic growth. Fibers grow in diameter by diffuse symplastic growth, but they elongate solely by intrusive apical growth penetrating the pectin-rich middle lamella that cements neighboring cells together. In contrast, vessel elements grow in diameter by a combination of intrusive and symplastic growth. We demonstrate that an abundant pectin methyl esterase (PME; EC 3.1.1.11) from wood-forming tissues of hybrid aspen (*Populus tremula* × *tremuloides*) acts as a negative regulator of both symplastic and intrusive growth of developing wood cells. When *PttPME1* expression was up- and down-regulated in transgenic aspen trees, the PME activity in wood-forming tissues was correspondingly altered. PME removes methyl ester groups from homogalacturonan (HG) and transgenic trees had modified HG methylesterification patterns, as demonstrated by two-dimensional nuclear magnetic resonance and immunostaining using PAM1 and LM7 antibodies. In situ distributions of PAM1 and LM7 epitopes revealed changes in pectin methylesterification in transgenic trees that were specifically localized in expanding wood cells. The results show that en block deesterification of HG by *PttPME1* inhibits both symplastic growth and intrusive growth. *PttPME1* is therefore involved in mechanisms determining fiber width and length in the wood of aspen trees.

When plant cells grow, they typically do so together (i.e. symplastically, attached by a common middle lamella; Evert, 2006). However, a few specialized cell types in primary plant tissues grow intrusively (i.e. between neighboring cells; Lev-Yadun, 2001). Although intrusive apical growth is a rare phenomenon, it is of great significance because it is the major determinant of phloem and xylem fiber length in angiosperm species (Larson, 1994; Lev-Yadun, 2001). Thus, it influences a major quality trait of commercial plant fiber raw materials, such as sisal, abaca, jute, flax, ramie, hemp, kenaf, and, perhaps most importantly, wood.

Most current research on cell growth is focused on cell wall plasticity and symplastic growth (for review, see Cosgrove, 2005). However, another important aspect, especially for intrusive growth, is cellular adhesion. Pectin is a major component of primary walls and likely to be important for both wall plasticity and cellular adhesion. A pectinaceous sheet, called the middle lamella, provides a contact interface between neighboring cells and the adhesion between cells depends on the formation of pectin intermolecular links between pectin molecules (Jarvis et al., 2003). Similarly, intramolecular links and composition of pectin influence wall plasticity (Ezaki et al., 2005; Proseus and Boyer, 2006; Derbyshire et al., 2007). One type of intermolecular link is created when calcium ions interact with the acidic form of homogalacturonan (HG) molecules (i.e. deesterified GalA units) to form rigid egg-box structures (Carpita and McCann, 2000). Formation of egg-box structures depends on the presence of a minimum of 20 deesterified GalA units along the HG chain, which can bind Ca^{2+} ions (Jarvis, 1984). HG is known to be synthesized and secreted in a highly methylesterified form (Zhang and Staehelin, 1992) and to be deesterified by pectin methyl esterases (PMEs) residing in the walls, resulting in the formation of free carboxylic residues (for review, see Pelloux et al., 2007). Both contiguous and random patterns of deesterification have been suggested as a result of PME action, the former leading to the formation of egg-box structures and wall stiffening and the latter inducing cell wall acidification and wall weakening (Micheli, 2001).

[1] The work was supported by grants from The Swedish Research Council Formas, the Swedish Research Council, the Wallenberg Foundation, the European Union Project Eden (QLK5–CT–2001–00443), and the Wood Ultrastructure Research Centre.

[2] This article is dedicated to the memory of Anna Siedlecka, who died tragically in spring 2004.

[3] Present address: CIRAD-CP, UMR PIA, F34398 Montpellier, France.

[4] Present address: Department of Botany, University of Białystok, Świerkowa 20 b, 15–950 Białystok, Poland.

* Corresponding author; e-mail bjorn.sundberg@genfys.slu.se.

The author responsible for distribution of materials integral to the findings presented in this article in accordance with the policy described in the Instructions for Authors (www.plantphysiol.org) is: Björn Sundberg (bjorn.sundberg@genfys.slu.se).

[W] The online version of this article contains Web-only data.

[OA] Open Access article can be viewed online without a subscription.

www.plantphysiol.org/cgi/doi/10.1104/pp.107.111963

Experimental data on the action of PMEs in planta are limited and many aspects of their functions and regulation remain to be elucidated. For instance, some studies in which PME expression has been modified indicate that it plays a role in wall stiffening and inhibition of wall plasticity (Wen et al., 1999; Hasunuma et al., 2004; Bosch et al., 2005), but others have found no evidence that it is involved in the regulation of symplastic growth and cell expansion (Tieman et al., 1992; Pilling et al., 2000, 2004). In addition, a pollen-specific PME (VANGUARD1) has been shown to be required for growth of the pollen tube (Jiang et al., 2005), and QUARTET1 (a PME) promotes wall loosening by making the pectin susceptible to degradation (Francis et al., 2006). It is not known whether these different results reflect different properties of particular PMEs or just underscore the complexity of the regulation of pectin methylesterification in plants. In spite of well-known implications of pectins in cell adhesion in plants (Jarvis et al., 2003; Francis et al., 2006), the role of the pectin network in intrusive growth is unclear and the mechanisms controlling intrusive growth are completely unexplored.

In wood-forming tissues of angiosperm species, the ultimate sizes of different cell types depend on a finely tuned balance of intrusive and symplastic growth, as explained below. The axial wood system of aspen (*Populus* spp.) consists primarily of fibers and vessel elements, organized in radial files, each of which differentiates from a fusiform initial in the vascular cambium (Mellerowicz et al., 2001). Any time a new file is to be initiated, the fusiform initial divides anticlinally. This division is oblique and shortens the initial's length (Fig. 1), but thanks to the intrusive apical growth, the length of the initial is maintained and may even increase as the cambium ages (Larson, 1994). The formation of new fibers and vessel elements then proceeds via a series of periclinal divisions, each followed by intrusive apical growth, of the fusiform initial and its derivative xylem mother cells. These processes result in a slight increase in the length of xylem mother cells within the cambial meristem (Larson, 1994). After the xylem mother cells leave the meristematic zone, the vessel elements do not elongate any further, but the developing fibers continue to elongate intrusively and markedly, their length increasing to 150% to 400% of the original xylem mother cell's length, depending on species (Wenham and Cusick, 1975; Larson, 1994; compare with Fig. 1). Thus, the extent of intrusive elongation is a major determinant of fiber length of angiosperm species, and elucidating the mechanisms involved in its regulation has clear fundamental and practical importance.

In contrast to apical elongation, the diameter growth of developing fibers and vessel elements is driven by diffuse growth of their entire radial walls (Mellerowicz et al., 2001). The most intense radial expansion occurs outside the meristem in the radial expansion zone. In this zone, developing fibers expand symplastically, but vessel elements expand more than adjacent cells by intrusive lateral growth of their radial walls followed by the displacement of adjacent cells. Thus, for the final vessel diameter, both symplastic growth and intrusive growth are important, whereas the fiber diameter is determined solely by symplastic growth.

We studied the role of a major native PME in cell growth in the wood-forming tissues of hybrid aspen (*Populus tremula* × *tremuloides*). Transgenic hybrid aspen trees were generated in which *PttPME1* expression was up- and down-regulated, with corresponding changes in PME enzyme activities. The trees with modified PME activity had altered degrees and patterns of HG methylesterification, vessel and fiber diameters, and fiber lengths. The results provide information demonstrating the role of PttPME1 in intrusive growth and support the hypothesis that HG methylesterification plays an important role in the regulation of wall plasticity.

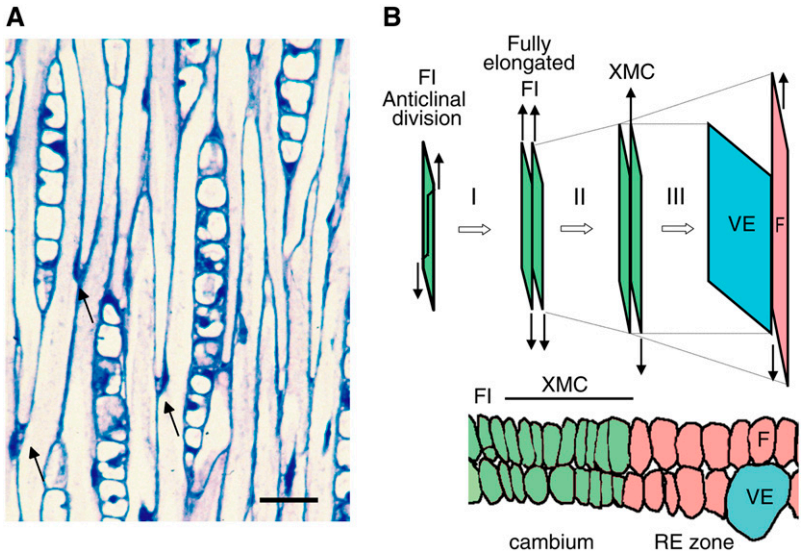

Figure 1. Intrusive tip growth during wood cell development. A, Tangential longitudinal section through the cambium showing intrusively growing cell tips (arrows). Scale bar = 50 μm. B, Diagram showing three developmental stages of cells elongating via intrusive growth, as seen in the radial longitudinal view (top) and the corresponding cross-sectional view (bottom). Stage I, intrusive apical growth results in elongation of fusiform initials (FI) following multiplicative anticlinal divisions in the cambium. Stage II, intrusive growth is responsible for elongation of xylem mother cells (XMC) in the cambial zone. Stage III, in the radial expansion (RE) zone, intrusive apical growth is responsible for the elongation of fibers (F), whereas vessel elements (VE) do not elongate outside the meristem.

RESULTS

Cloning and Expression of *PttPME1*

A 2,149-bp *PttPME1* cDNA (accession no. AJ277547) was isolated by screening an aspen cDNA library of cambial region tissues (Sterky et al., 1998). The 1,739-bp open reading frame was 96.8% identical to the open reading frame of its best hit, *Populus trichocarpa* gene model *grail3.0029000401* at scaffold 29:48410-43182 (http://genome.jgi-psf.org/Poptr1_1/Poptr1_1.home.html) and it encoded a pre-proprotein of 62.9 kD with high similarity to most plant PME precursors. It carried a signal peptide flanked by a transmembrane domain (Dorokhov et al., 2006) with a predicted cleavage site at position Ala-46 (von Heijne, 1986) and a potential proteolytic cleavage site in the vicinity of Pro-267 (Micheli, 2001) that would putatively release a mature protein of 34 kD with an isoelectric point of 8.88. Two potential *N*-linked glycosylation sites, specified by the sequence Asn-X-Ser/Thr, were found in the N-terminal Pro region (Fig. 2A).

Expression of *PttPME1* was investigated in stem tissues active in secondary growth and during dormancy using a *PttPME1*-specific probe. Transcripts were most abundant in the primary-walled developing wood cells (i.e. the cambial meristem and its expanding and elongating derivatives; Fig. 2B). These are the tissues where cell growth takes place during wood development, and they were used in all further molecular and chemical analyses. No expression was detected in the nongrowing dormant cambium, indicating that *PttPME1* expression is related to cell growth.

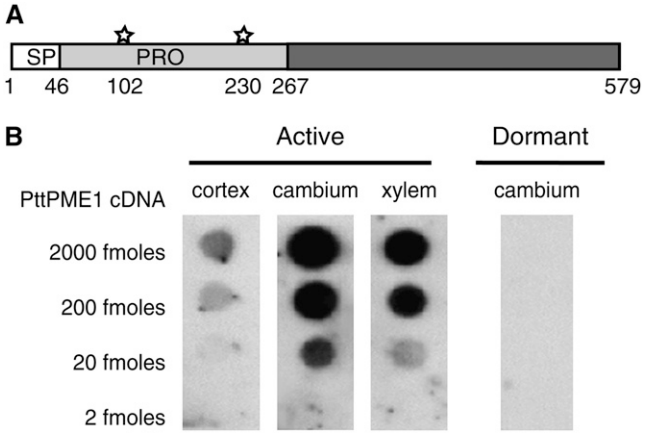

Figure 2. Characterization of *PttPME1*. A, Deduced peptide of PreProPttPME1. SP, Signal peptide; PRO, pro-protein N terminus. Two hypothetical glycosylation sites are marked by stars. B, Reverse-northern dot blot with the *PttPME1*-specific probe showing *PttPME1* expression in the periderm, secondary phloem (denoted cortex), primary phloem, cambium, and expanding/elongating wood cells (denoted cambium), in secondary-walled developing wood cells (denoted xylem) during activity, and in the cambium during dormancy.

Generation of Transgenic Aspens with Modified *PttPME1* Expression

To investigate the importance of the degree of HG methylesterification for intrusive and symplastic growth, and hence xylem cell length and width, *PttPME1* cDNA was expressed in aspen under the control of the constitutive 35S promoter. Regeneration and multiplication of transgenic lines proved to be difficult and only seven transgenic lines were obtained. In addition, the gene-specific 3′-fragment of *PttPME1* was introduced to aspen in antisense orientation. Unfortunately, none of the antisense lines that were regenerated exhibited significantly reduced *PttPME1* transcript levels (data not shown). However, five sense lines had reduced *PttPME1* transcript levels and two showed increased levels of *PttPME1* expression, as determined by quantitative reverse transcription (RT)-PCR (Fig. 3A). The lines did not exhibit major changes in plant height or stem anatomy as observed by light microscopy (data not shown). Southern-blot analysis revealed that the lines resulted from independent transformation events and each had between one and six inserts (Fig. 3B).

PttPME1 Affects Wood Cell Expansion in Transgenic Lines

The radial expansion of wood cells depends on the plasticity of cell walls during symplastic growth and, for vessel elements, also on dissolution of the middle lamella during the intrusive lateral growth. The length of wood fibers, however, depends solely on intrusive growth. To evaluate the effect of *PttPME1* expression on xylem cell growth, individual cells were measured in macerates of mature wood from the two most strongly up-regulated lines (lines 7 and 2B), the most strongly down-regulated line (line 5), and one slightly down-regulated line (line 8). Fiber length was found to be inversely correlated to *PttPME1* expression levels (Fig. 4, A and B); approximately 50% increases and reductions in expression levels leading to approximately 5% to 10% reductions and increases in fiber length, compared with the wild type, respectively. The length of vessel elements was not affected. However, the vessel tail length was affected in lines 5 and 2B in the same manner as the fiber length (data not shown). The growth in width of both fibers and vessel elements was clearly stimulated by a reduction in *PttPME1* expression, but no consistent effects of increased *PttPME1* expression were observed (Fig. 4). The increases in fiber and vessel width were in the range 10% to 15%. Taken together, these data demonstrate that modification of *PttPME1* expression affects symplastic and intrusive cell growth of fibers and vessels in the secondary xylem of hybrid aspen.

NMR and Immunochemical Analysis Reveals Changes in the Degree and Pattern of HG Methylesterification in Transgenic Lines

To determine the degree of methylesterification (DM) of HG in the *PttPME1* lines with altered cell

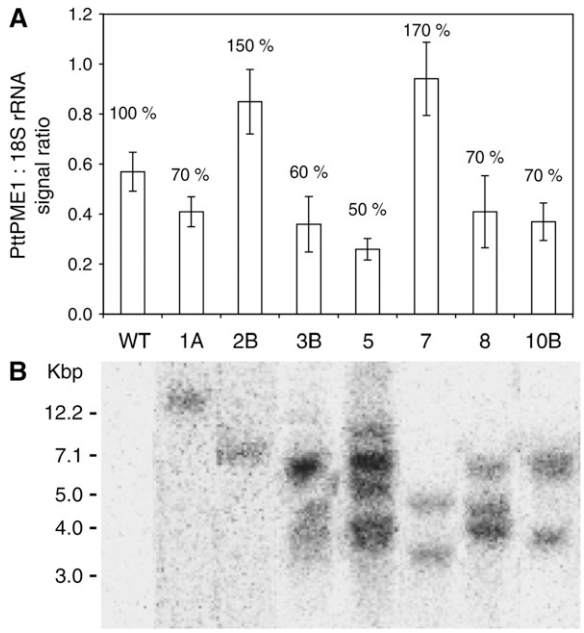

Figure 3. Characterization of transgenic lines with 35S:*PttPME1* cDNA. A, Quantitative RT-PCR analysis of *PttPME1* expression showing the ratio of signals from *PttPME1* and *18S rRNA*. Expression levels (percent) relative to the wild type are indicated above the bars. Bars = ±SE; three technical replicates, each sample containing tissues pooled from four to eight trees. B, Transgene integration pattern analyzed by Southern blotting. The number of bands shows the number of inserts.

growth, we extracted pectins with buffers containing cyclohexane diamine tetraacetic acid (CDTA) and analyzed them using a two-dimensional NMR procedure. Because transgenic effects might concern only particular pectin fractions, we used 10, 30, or 50 mM CDTA buffer to extract different fractions of HG for the NMR experiments. The resonances from methylesterified and nonmethylesterified HG were identified using a method that combines the resonances from ^{1}H and ^{13}C atoms (Fig. 5). H5 resonances of methylesterified and nonmethylesterified galacturonan were resolved completely and used to quantify differences between transgenic lines and wild-type trees. In addition, H4 resonances of methylesterified and nonmethylesterified galacturonan could also be distinguished. Although these signals were not completely resolved, they served as independent controls for the observed differences in H5 signals (data not shown). In the wild type, the DM varied between 44% to 57% for the different CDTA fractions. The down-regulated line 5 had a higher DM than the wild type in all HG fractions, whereas the up-regulated lines 2B and 7 had a lower DM. In the up-regulated line 7, changes were smaller than in line 2B and most pronounced in the 10 mM CDTA fraction. The difference between transgenic lines and the wild type was in the range of −10% to +25% (in the 50 mM CDTA fraction), and proven to be statistically significant by multiple linear regression analysis (Box et al., 1978; Supplemental Fig. S1).

The HG methylesterification patterns in wild-type and transgenic trees were further explored immunohistochemically using monoclonal antibodies that specifically bind to HG with different distributions of methyl ester groups. This approach allows in situ visualization of specific pectin epitopes and is capable of detecting modifications in specific tissues and cell types that may be diluted in NMR analysis of ground tissue samples. JIM5 and JIM7 have often been used to evaluate DM. However, JIM5 and JIM7 can bind HG with a wide range of different methylesterification patterns (Willats et al., 2000; Clausen et al., 2003). Therefore, we used PAM1 and LM7 antibodies, which have been demonstrated to bind to highly specific HG epitopes; PAM1 reacts with 30 contiguous deesterified HG units and LM7 with four consecutive deesterified

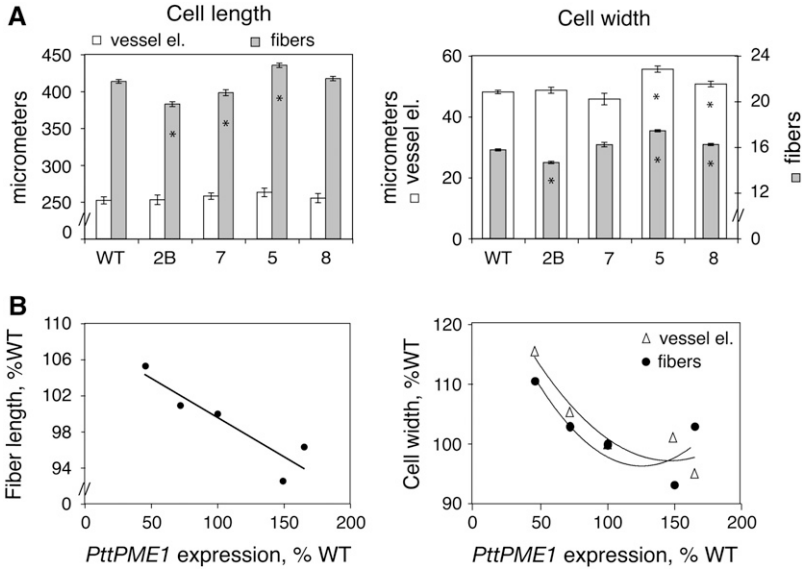

Figure 4. A, Length and width of fibers and vessel elements in *PttPME1* up-regulated (2B and 7) and down-regulated (5 and 8) lines, and wild-type plants. Bars = SE; *n* = approximately 1,000 for fibers and 200 for vessel elements from five different trees; stars indicate averages significantly different from the wild type (Duncan multirange test; $P \leq 0.05$). B, Relationship between fiber length or xylem cell width and *PttPME1* expression levels. Best-fit lines were drawn using linear or polynomial second-order functions.

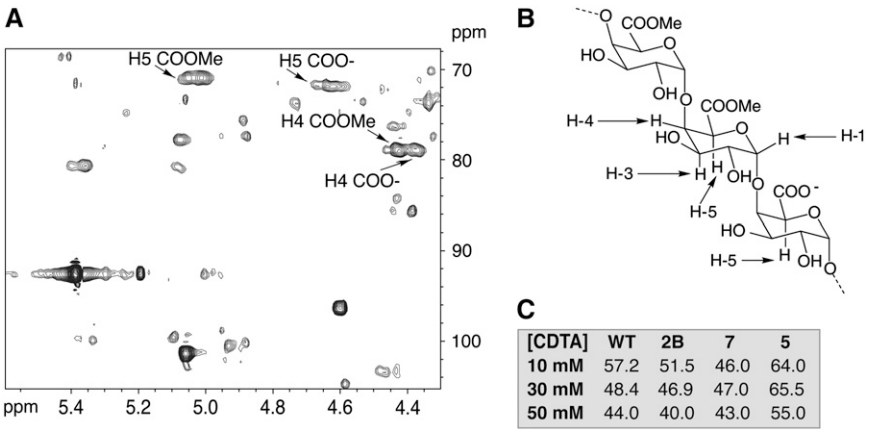

[CDTA]	WT	2B	7	5
10 mM	57.2	51.5	46.0	64.0
30 mM	48.4	46.9	47.0	65.5
50 mM	44.0	40.0	43.0	55.0

Figure 5. ^{1}H-^{13}C two-dimensional NMR analysis of CDTA extracts from wood-forming tissues of wild-type aspen and transgenic lines with up-regulated (2B and 7) or down-regulated (5) *PttPME1* expression. A, Example of ^{1}H-^{13}C HSQC spectrum showing effects of methylesterification on resonances of H4 and H5 protons of GalUA. Methylesterification shifted the H4 peak from 4.38 ppm to 4.43 ppm, and the H5 peak from 4.63 ppm to 5.05 ppm. B, Structure of GalUA. C, DM of HG in pectin fractions extracted with 10, 30, and 50 mM CDTA in transgenic lines based on the integration of H5 peaks. The table shows averages of two biological replicates; each replicate sample contained pooled tissues from four to eight trees and was analyzed two times. Linear multivariate modeling showed that the differences between genotype and the wild type were significant ($P \leq 0.05$; Supplemental Fig. S1).

HG units in sparsely methylesterified HG (Clausen et al., 2003).

In situ distribution of PAM1 and LM7 epitopes was visualized in wild-type and transgenic lines (Fig. 6). The PAM1 epitope was detected at low levels and often observed at junction points where cell corners initially meet and separate in later developmental stages via the formation of intracellular spaces (Fig. 6B). Labeling was markedly enhanced in the *PttPME1*-overexpressing line 2B, specifically in the radial expansion zone where it was found across broader cell wall areas (Fig. 6A, arrow). The LM7 epitope was observed only in the *PttPME1* down-regulated line 5, in which weak labeling was detected (often localized to cell corners), in the zone of xylem radial cell expansion (Fig. 6F). A dot-blot experiment confirmed the differential abundance of the PAM1 epitope and showed the dependence of its occurrence on the level of *PttPME1* expression (Fig. 7, A and B). No LM7 signal was detected by dot blotting, confirming the low abundance of this epitope (data not shown).

To find out whether modified *PttPME1* expression in transgenic lines induced any changes in the amount of pectins, we resuspended crude cell wall preparations in either water or 50 mM CDTA-containing buffer and estimated the total uronic acid content in slurry using a modified Blumenkrantz and Asboe-Hansen method (Kim and Carpita, 1992). This procedure allows measurement of uronic acids of pectin chains completely in solution after CDTA extraction (approximately 40%) as well as the ones in pectin chains still attached at some point to the cell wall network

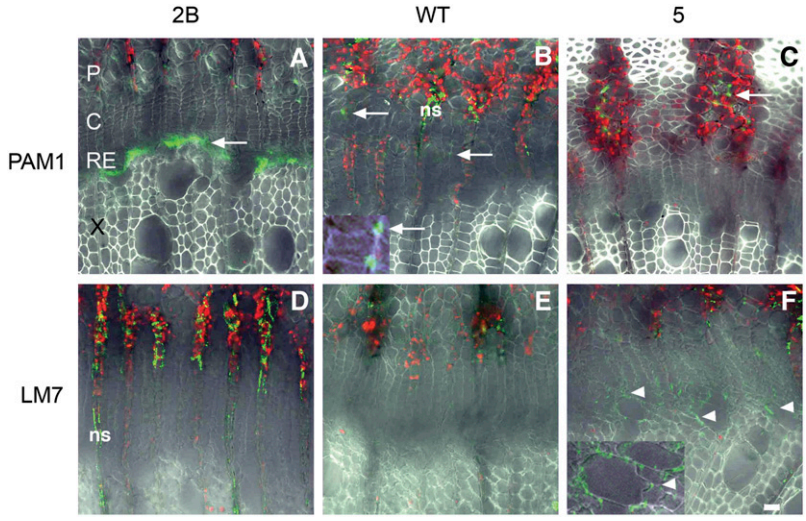

Figure 6. Immunolocalization of HG epitopes with different methylesterification patterns (green) in the wood-forming tissues of the wild type (B and E), up-regulated (2B, A and D), and down-regulated (5, C and F) *PttPME1* lines. Inserts show PAM1 (arrows) and LM7 (arrowheads) signals at cell corners. Negative controls were prepared without primary antibodies and generated no signals except nonspecific signals (ns) in the air-filled spaces of the rays, as also shown in the experimental sections in B and D. C, Vascular cambium; P, phloem; RE, xylem radial expansion zone; the red signal originates from the autofluorescence of chlorophyll. Scale bar (shown in F) = 20 μm.

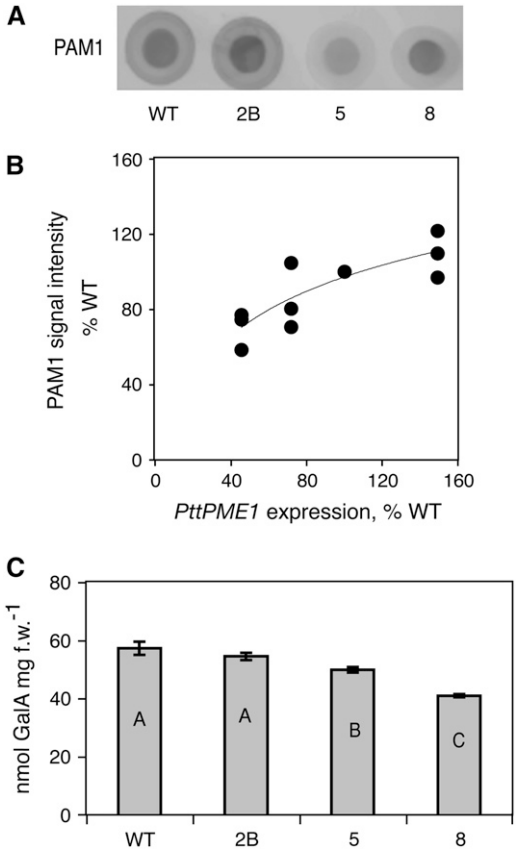

Figure 7. Analysis of CDTA-extracted and total CDTA-accessible pectin in up-regulated (2B) and down-regulated (5 and 8) *PttPME1* lines. A and B, Immunodot blots using the PAM1 monoclonal antibody. Equal loads of CDTA-extracted uronic acid from each line were dot blotted onto nitrocellulose in a dilution series and probed with PAM1. A, Example of a dot-blot pattern. B, Relationship between the quantified PAM1 signal from a dilution series and *PttPME1* expression levels. A logarithmic function was used to draw a best-fit trend line. Each sample contained tissues pooled from four to eight trees; three technical replicates. C, Total CDTA-accessible uronic acid content as determined by the modified Blumenkrantz and Asboe-Hansen procedure (Kim and Carpita, 1992) in cell slurry suspended in 50 mM CDTA buffer. GalA was used for the calibration curve. Bars = ±SE; n = six technical replicates; each sample contained tissues pooled from four to eight trees. Means accompanied by different letters are significantly different (Duncan multirange test; $P \leq 0.05$).

(approximately 60%). We found that PME-down-regulated lines had reduced levels of CDTA-accessible pectin, indicating a decreased level of Ca^{2+}-bound HG (Fig. 7C), whereas the water-accessible uronic acid levels were not significantly affected (data not shown).

Taken together, data from the physical and immunochemical analyses demonstrate that altering the expression of *PttPME1* in transgenic trees altered the DM in an expected fashion. Overexpression of *PttPME1* led to contiguous HG demethylesterification, whereas its deficiency led to a novel pectin epitope with a sparse methylesterification pattern. The in situ visualization data further demonstrate that the changes in the methylesterification patterns in the transgenic lines coincided with the location of radial expansion.

Altered *PttPME1* Expression Changes PME Activity and the Pattern of PME Isoforms in Transgenic Lines

The effect of altered expression of *PttPME1* on overall PME enzyme activity was examined in the wall-bound fraction (1 M NaCl extractable) and the soluble protein fraction (Fig. 8, A and B). The wall-bound fraction contained far more activity than the soluble fraction, but activities in both fractions were affected by the changes in *PttPME1* expression in transgenic lines. In line 5, activity in the wall-bound fraction was only 10% of wild-type levels, whereas it was increased in line 2B to 130% of wild-type levels. A correlation between *PttPME1* expression and PME activity was found (Fig. 8B), indicating that the *PttPME1* gene

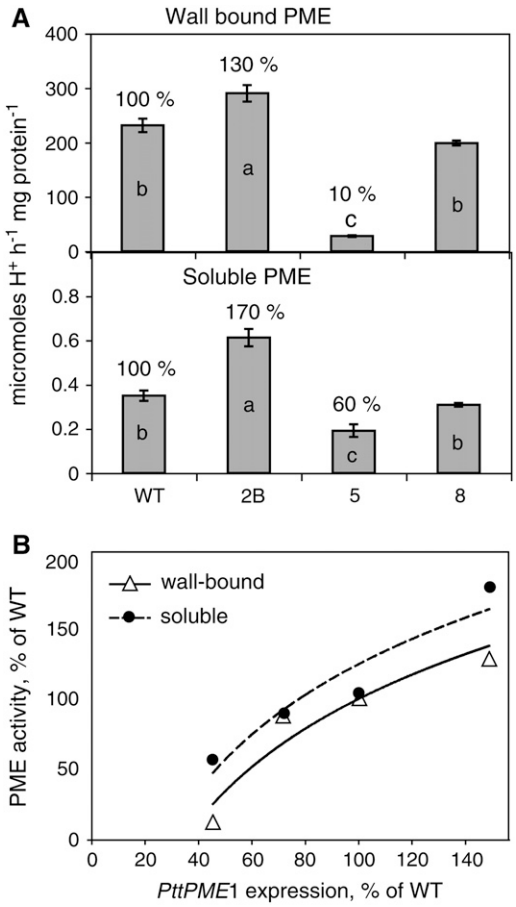

Figure 8. A, PME activity in wall-bound and soluble protein fractions of transgenic lines with up-regulated (2B) and down-regulated (5 and 8) *PttPME1* expression. Activity levels (percent) relative to the wild type are indicated above the bars. Bars = ±SE; n = six technical replicates, each sample containing tissues pooled for four to eight trees. Means accompanied by different letters are different (Duncan multirange test; $P \leq 0.05$). B, Relationship between *PttPME1* expression levels and PME activities. Best-fit lines were produced using a logarithmic function.

encodes an enzyme with PME activity, as predicted from the sequence analysis.

There are many PME isoforms in wood-forming tissues (Guglielmino et al., 1997a; Micheli et al., 2000). Analysis of PME activity in gels following isoelectric focusing of the wall-bound protein fraction revealed large differences in staining for the neutral isoforms centered around pI 7.3 (N3), which were the most abundant PME isoforms in the developing wood of the wild type (Fig. 9). In line 5, in which *PttPME1* expression was suppressed, the N3 isoforms almost disappeared, and in samples from the overexpressing line 2B, the signal from the band corresponding to the N3 isoform was increased. In addition, basic isoforms with pIs around 8.5 (B2 and B3) covaried with N3, although changes in transgenic lines were not as large. The mature form of the PttPME1 protein (lacking the signal peptide and the Pro region) has a predicted pI of 8.88 and could correspond to B3. We identified no mature PMEs with a neutral pI corresponding to the N3 isoform in the EST database from wood-forming tissues (Supplemental Table S1). However, the uncleaved PttPME1 and the corresponding protein of *P. trichocarpa* encoded by *grail3.0029000401* would give rise to a neutral isoform with a pI of 7.28. Thus, the uncleaved PttPME1 enzyme may represent the major N3 isoform revealed by isoelectric focusing, although additional work is required for a firm conclusion regarding this possibility.

In line 5, we expect other similar *PME* genes to be cosuppressed with *PttPME1*. Searches by BLAST in the *Populus* genome database revealed 11 gene models sharing at least one 22-nucleotide stretch with *PttPME1* (data not shown), which are all likely candidates to be affected. Consistent with this expectation, isoelectric focusing revealed a disappearance of additional PME isoforms in this line, such as pI 4.5 (new) and 6.8 (N2; Fig. 9). Thus, the different pattern of isoforms present in line 5 cannot be attributed solely to *PttPME1*, but most likely to similar PMEs affected in concert by the cosuppression mechanism.

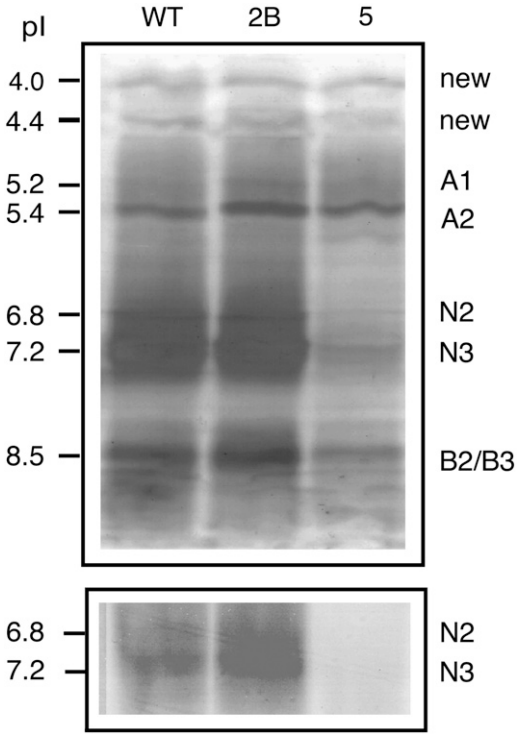

Figure 9. Results of isoelectric focusing of PME activity in the wall-bound protein fractions extracted from up-regulated (2B) and down-regulated (5) *PttPME1* lines demonstrating changes in neutral and basic isoforms. Samples were calibrated to 200 μg (top) or 100 μg (bottom) of dried cell walls. Designations of previously described PME isoforms (Micheli et al., 2000) are shown on the right. Samples were pooled for four to eight trees/line.

DISCUSSION

PttPME1 Is an Abundant PME Involved in Xylogenesis

PME is a ubiquitous enzyme in plants, encoded by 66 genes in Arabidopsis (*Arabidopsis thaliana*), most showing tissue- and stress-specific expression patterns (Louvet et al., 2006; Pelloux et al., 2007; http://www.afmb.cnrs-mrs.fr/CAZY/CE_8.html). In the *Populus* genome, 89 gene models with similarity to plant PMEs have been identified (Geisler-Lee et al., 2006; Pelloux et al., 2007; http://genome.jgi-psf.org/Poptr1_1/Poptr1_1.home.html). Fourteen of them have corresponding ESTs in libraries from wood-forming tissues and some showed distinct expression patterns during wood development in cDNA microarray studies (Pelloux et al., 2007). With gene-specific probes, *PttPME1* was found to be more expressed in the primary- than in secondary-walled developing xylem (Fig. 2B), indicating that the corresponding protein is important in the early stages of xylogenesis when cell growth takes place. Modified expression of *PttPME1* in transgenic trees resulted in substantial changes in both wall-bound and soluble PME activities (Fig. 8), demonstrating that the gene encodes an important bona fide PME. Isoelectric focusing of cell wall-bound PMEs detected a total of eight isoforms with pI values ranging from 8.5 to 4.0 (Fig. 9) in accordance with data presented by Guglielmino et al. (1997a) and Micheli et al. (2000). The neutral isoforms centering on pI 7.3 (N3) were the most abundant and they were also the isoforms that were most affected by modified *PttPME1* expression, together with the less abundant B2/B3 isoforms (Fig. 9). The predicted pI of mature PttPME1 protein is close to that of B2/B3, indicating that the mature PttPME1 may contribute to these isoforms. Analysis of predicted pIs of wood-expressed PMEs published by Geisler-Lee et al. (2006) did not detect any obvious candidate for a neutral isoform among the mature PMEs (Supplemental Table S1). However, the predicted pIs of Pro-PME1 matched that of N3, suggesting that both cleaved and uncleaved forms accu-

mulate in the cell wall. In support of this hypothesis, a peptide from a Pro region of PttPME1 protein has been identified in the aspen cell wall-bound proteome (R. Nilsson and G. Wingsle, personal communication). The Pro region of group 2 (former type I) PMEs contains a PME inhibitor (PMEI) domain that participates in PME secretion to the cell wall and is cleaved off, most likely outside the protoplast, to release the esterase domain (Micheli, 2001; Bosch et al., 2005; Di Matteo et al., 2005; Dorokhov et al., 2006; Pelloux et al., 2007). The PMEI domain of NtPPME1 inhibited activity of the esterase domain when coexpressed in tobacco (*Nicotiana tabacum*), suggesting a role of PMEI as an intramolecular inhibitor of PME activity (Bosch et al., 2005). However, in flax (*Linum usitatissimum*), PMEs with M_rs corresponding to uncleaved forms exhibited activity in native gels (Al-Qsous et al., 2004). Therefore, we suggest that uncleaved PttPME1 contributed to N3. Sequencing of different PME isoforms will be required to clarify this point.

PttPME1 Stabilizes Pectin Network

If PttPME1 is an important PME in wood-forming tissues, alterations in its activity should change the degree and pattern of HG methylesterification. In accordance with this expectation, we found changes in HG DM in CDTA-extracted pectin and in the methylesterification pattern detected with antibodies (Figs. 5–7). Up-regulation of *PttPME1* resulted in a small but significant decrease in average DM and an increase in en block deesterification detected by PAM1. This indicates that PttPME1 has processive activity in planta, which has been frequently ascribed to plant basic PMEs (Catoire et al., 1998; Micheli, 2001). Suppression of PttPME1 (and possibly similar PMEs) in aspen wood-forming tissues resulted in a lower amount of galacturonan (Fig. 7C) as was also observed in PME-suppressed tomato (*Solanum lycopersicum*) fruit (Tieman et al., 1992). This probably relates to the occurrence of more sparsely esterified epitopes, such as LM7, and a lower amount of egg-box complexes that stabilize HG (Jarvis, 1984; Baluška et al., 2002), hence a pectin that is more susceptible to degradation by pectin lyases and polygalacturonases (Limberg et al., 2000; van Alebeek et al., 2002; Wehr et al., 2004). In summary, PttPME1 appears to be an important enzyme in the generation of egg-box structures and stabilizing pectins in the cell wall during wood development.

PttPME1 Inhibits Symplastic and Intrusive Growth

It has been postulated that HG methylesterification levels and patterns are important determinants of cell wall plasticity and thus diffuse symplastic growth (Goldberg et al., 1986; Micheli, 2001). Supporting this hypothesis, several studies have found gradients of decreasing HG methylesterification levels and increasing PME activities from expanding to maturing tissues (Goldberg et al., 1986; Alexandre et al., 1997; Guglielmino et al., 1997b; Femenia et al., 1998; Fujino and Itoh, 1998; Parre and Geitmann, 2005). We found that down-regulation of *PttPME1* (and possibly similar PMEs) stimulated radial expansion in both vessel elements and fibers (Fig. 4), indicating that these PMEs are negative regulators of wall plasticity in developing wood cells. This agrees with many observations in other cell types in different species, regarding PMEs from both plant and fungal sources (Wen et al., 1999; Hasunuma et al., 2004; Bosch et al., 2005; Derbyshire et al., 2007). Our results support the hypothesis that wall stiffening involves Ca^{2+}-mediated pectin gelation and immobilization, and that *PttPME1* is involved in these processes.

Interestingly, suppression of *PttPME1* in line 5 (Fig. 9) resulted in the appearance of a sparsely methylesterified LM7 epitope (Clausen et al., 2003; Fig. 6F). This suggests that other PMEs active in developing wood tissues deesterify pectin by a multiple attack mechanism (Catoire et al., 1998). These PMEs might contribute to wall loosening mediated by pectin-degrading polygalacturonases as observed in the pollen tube in *Solanum chacoense* (Parre and Geitmann, 2005). That an acidic PME is required for pectin breakdown promoting wall loosening in planta has been recently shown by cloning of the *QUARTET1* gene (Francis et al., 2006). Thus, it seems likely that differences in the balance of acidic and neutral PMEs across the cambial meristem and expanding xylem cells in *Populus* (Micheli et al., 2000) are important for developmental patterns of cell expansion in developing wood. In *Populus*, expression of acidic PME isoforms of pI 5.2 (A2) was recorded in cambial cells, whereas the expression of neutral N3 isoforms (likely *PttPME1*) lasted until later stages of xylogenesis in the radial expansion zone (Micheli et al., 2000). Moreover, microarray analysis of gene expression across the cambial meristem (Schrader et al., 2004) revealed two distinct patterns for *PME* genes, with peak expression either in the center of the meristem or close to the exit from the meristem and the beginning of the radial expansion zone, as in the case of *PttPME1* (Pelloux et al., 2007).

The observed effects of transgenic modification of *PttPME1* expression levels on fiber length in aspen demonstrate the involvement of PME activity in intrusive apical growth of wood fibers (Fig. 4). High PME activity inhibited, while low activity stimulated, fiber elongation. Intrusive tip growth requires: (1) dissolution of the middle lamella; (2) yielding of the wall between adjacent cells to create space for the growing tip; and (3) wall biosynthesis at the fiber tip. *PttPME1* (and possibly similar PMEs) may be involved in all of these processes, but we propose that its major impact is through modification of the middle lamella leading to changes in the degree of cellular adhesion. By generating methyl-free HG stretches, thus creating stiff pectin-calcium-pectin structures and stabilizing pectin network, PttPME1 would strengthen cellular adhesion and hinder intrusive growth. Similar

to PttPME1, PME isoforms in flax and tomato had a cell adhesion-promoting role (Lamblin et al., 2001; Orfila et al., 2001; Lacoux et al., 2003). Conversely the appearance of the LM7 epitope (Fig. 6F), a marker of cell separation (Willats et al., 2000), suggests that residual PME activities might assist fiber intrusive growth. A PME protein has been localized at cell junctions in wood-forming tissues of poplar (Guglielmino et al., 1997a), where it may directly regulate methylesterification and thus affect cellular adhesion and intrusive fiber growth. Other factors important for cell adhesion, including pectin acetylation (Liners et al. 1994), the content of HG (Rhee and Somerville, 1998; Atkinson et al., 2002; Bouton et al., 2002; Leboeuf et al., 2005; Francis et al., 2006), rhamnogalacturonan II (Iwai et al., 2002), arabinan (Iwai et al., 2001, Orfila et al., 2001), and other adhesion-regulating genes (Shi et al., 2003; Takahata et al., 2004; Singh et al., 2005), could also play an important role in fiber elongation. An understanding of intrusive growth opens a number of possibilities for marker-assisted selection and biotechnological manipulation of the length of wood fibers, as well as other economically important fibers that elongate via intrusive growth, including sisal, abaca, jute, flax, ramie, hemp and kenaf (for review, see Lev-Yadun, 2001). Several genetic approaches have been taken to select long-fiber tree varieties, but little is known about genes responsible for this trait. A cellulase, the class of enzyme traditionally regarded as the wall plasticity regulator, was initially reported to have a fiber length-increasing role in aspen (Shani et al., 1999), but this effect was not confirmed in a subsequent study (Shani et al., 2004). Ectopic overexpression of expansin in aspen did not increase the fiber length (Gray-Mitsumune et al., 2007), suggesting that techniques targeting wall plasticity alone may not be sufficient to enhance the intrusive growth of wood fibers. Recently, a transgenic approach was used to increase the GA content in developing wood by ectopic expression of GA 20-oxidase, which resulted in an 8% increase in wood fiber length (Eriksson et al., 2000). Transgenic trees showed altered transcript levels for a number of cell wall biosynthetic and modifying enzymes, including pectin-acting genes (Israelsson et al., 2003). These findings suggest that pectin metabolism is a promising target for biotechnological attempts to modify fiber length.

MATERIALS AND METHODS

Plant Material

Hybrid aspen (*Populus tremula* × *tremuloides*), clone T89, was grown in a greenhouse under a photoperiod of 18 h with natural light supplemented with metal halogen lamps. The temperature was 22°C/15°C (day/night), and the trees were watered daily and fertilized once a week with a nutrient solution (Superba; Yara AB). Trees were grown to a height of 1.5 m. Dormancy was induced by natural autumn photoperiods in the unheated greenhouse and tissues from these trees were sampled at the quiescent stage of dormancy (Romberger, 1963).

Samples containing cambium and the radial expansion zone of developing wood for molecular and chemical analyses were collected from internodes with well-advanced secondary growth by peeling the bark and scraping the exposed tissues from the phloem side as described by Gray-Mitsumune et al. (2004). Dormant cambium was scraped from the exposed wood side. Collected tissues were ground in liquid nitrogen with a mortar and pestle and the powdered tissues were stored at −80°C until use.

Cloning of *PttPME1* cDNA

Two degenerate primers (5′-AMTGGAACARTCGATTTCATYTTCGG-3′ and 5′-GAATATTCCTTCCAHGGMCGACCAARATAC-3′) were used to amplify a 200-bp *PME* fragment from genomic DNA. A λt22a cDNA library, prepared from the cambial region (Sterky et al., 1998), was screened under high stringency with the 200-bp probe. Positive inserts were cloned in pBluescript SK (Stratagene) and sequenced on both strands.

RNA Extraction and *PttPME1* Expression Analyses

Total RNA was extracted from powdered tissue using the hot CTAB method (Chang et al., 1993) and purified with RNeasy plant mini kit columns (Qiagen).

Reverse-Northern Dot Blotting

A 3′-untranslated region fragment of *PttPME1* cDNA corresponding to nucleotides 1,772 to 2,112 of the accession AJ277547 was verified as *PtPME1* specific by a BLAST search of the *Populus* genome database (http://genome.jgi-psf.org/Poptr1_1/Poptr1_1.home.html). Serial dilutions of DNA corresponding to this fragment were denatured in 0.4 N NaOH and spotted onto a positively charged nylon membrane (Amersham) using a vacuum manifold (Schleicher and Schuell). The cDNA probe was prepared as described by Micheli et al. (1998), purified on Sephadex G50 (Pharmacia), and added to hybridization buffer (Church and Gilbert, 1984) at a concentration of 8.8 10^6 cpm/mL. Following hybridization and high-stringency washes, autoradiographs were obtained and scanned using Photoshop (Adobe Systems). Images were analyzed using National Institutes of Health Image 1.57 software (Wayne Rasband; NIH).

Quantitative RT-PCR

Total RNA was treated with DNase and reverse transcribed using random hexamer primers (50 ng/μL) and the Moloney murine leukemia virus reverse transcriptase (Roche Diagnostics). First-strand cDNA was used as a template in PCR using the primer set 5′-ATTTCATTTTCGGCAATGCT-3′ and 5′-GCGCCACGAAGAGAATACAT-3′, which yields a 516-bp product specific for sense mRNA. PCR was optimized (32 cycles of 94°C for 30 min, 62°C for 30 min, and 72°C for 30 min) according to recommendations for the Quantum RNA kit (Ambion).

Generation of Transgenic Aspen

Full-length *PttPME1* cDNA (sense construct) or its 3′ gene-specific fragment (antisense construct) was cloned into the binary vector pBI121 (CLONTECH). The vector was transferred to aspen as described previously (Gray-Mitsumune et al., 2007) via *Agrobacterium tumefaciens* strain GV3101 (Koncz and Schell, 1986). Kanamycin-resistant lines were clonally propagated in vitro and planted in the greenhouse.

Southern-Blot Analysis

Genomic DNA was extracted from young shoots using the hot CTAB method (Doyle and Doyle, 1989), with modifications described by Fang et al. (1992), digested with *Hin*dIII, separated on a 0.7% agarose gel, and transferred to a Hybond-N+ membrane (Amersham-Pharmacia Biotech) under alkaline conditions. The membrane was probed at high stringency with a fragment specific to the *NPT*II gene present in the vector. Radioactivity was analyzed by a phosphor imaging system (GS-525, Molecular Imager; Bio-Rad).

Wood Cell Measurements

Wood from internode 40, counting from the top, was macerated in an acetic acid-peroxide cocktail until single cells were obtained (Berlyn and Miksche,

1976). Cells were stained with toluidine blue O and examined under an Axioplan 2 microscope (Zeiss). Vessel element length was measured without tails. Their tails, if present, were measured separately. Extended focus images were captured by an AxioVision camera (Zeiss) and cells were measured directly on the computer screen.

Pectin Analysis

NMR

For NMR analyses, pectins were extracted from tissue powders with three different buffers containing 50 mM Tris-HCl (pH 7.2) and either 10, 30, or 50 mM CDTA. The extraction was continued for 10 min at 95°C with intermittent vortex mixing and the sample was then centrifuged at 10,000 rpm for 10 min. All samples were lyophilized and dissolved in D_2O. Prior to NMR analysis, pH was set to 6.1.

Gradient-enhanced Heteronuclear Single Quantum Coherence (ge-HSQC) ^{1}H-^{13}C spectra were acquired using a Bruker DRX spectrometer (Bruker Biospin) operating at a proton frequency of 600 MHz, using a 5-mm TXI probe equipped with Z gradients. NMR measurements were recorded at 75°C to ensure sufficient mobility of the pectin polymer. The ge-HSQC ^{1}H-^{13}C two-dimensional NMR spectra (Kay et al., 1992) were collected using sine-shaped gradients for the coherence selection. Sweep widths of 13 ppm and 98 ppm were used in the ^{1}H and ^{13}C dimensions, respectively. For each NMR experiment, 32 to 88 scans were collected using a relaxation delay of 1.5 s for each of the 128 t_1 increments.

DM was determined by integrating the spectral regions of H5 for the nonmethylesterified and methylesterified peaks that were fully resolved, as opposed to the other resonances. The assignments correspond to proton resonances previously reported (Grasdalen et al., 1988; Rosenbohm et al., 2003). Corresponding ^{13}C resonances were identified by recording two-dimensional ^{1}H-^{13}C spectra of 95% methyl-esterified citrus pectin and poly GalUA (both from Sigma-Aldrich).

For the final analysis, duplicate biological replicates were prepared using different pools of trees, resulting in 24 samples (i.e. two biological replicates for all fractions and lines). Results were evaluated by multiple linear regression, where CDTA concentration was a quantitative factor, genotype was a qualitative factor, and DM was the response (Box et al., 1978). Three models were evaluated separately comparing each transgenic line with the wild type using MODDE Version 7.0.0.1 (Umetrics AB).

Immunochemical Analyses

For other procedures, pectins were extracted from tissue powders with the hot buffer containing 50 mM CDTA, as above. The immunodot-blot procedure was according to Willats and Knox (1999). Equal amounts of uronic acids from each line were dot blotted onto nitrocellulose in a 5× dilution series and probed with LM7 and PAM1 monoclonal antibodies, followed by a secondary anti-rat antibody conjugated to peroxidase or, in the case of PAM1, by anti-His monoclonal antibody and a tertiary anti-mouse antibody coupled to peroxidase (all from Sigma). All monoclonal antibodies were gifts from Dr. W.G.T. Willats and Dr. J.P. Knox. The peroxidase product was detected with ECL Plus reagents (Amersham) and quantified with the Typhoon scanner 9400 (Amersham) in fluorescence mode using 415-nm excitation and 455-nm detection wavelengths.

For immunolocalizations, stem internodes 15 to 20, counting from the top, were free-hand sectioned and processed as described by Willats et al. (2001). Negative controls were treated without primary antibodies or without any antibodies (autofluorescence controls). Sections were examined by confocal laser microscopy (Zeiss LSM 510). Sections were excited with 488-nm light and FITC signals were detected between 505 and 530 nm. Chlorophyll autofluorescence signals were detected above 650 nm and superimposed onto the transmitted light signals for anatomical detail. All samples that were compared were scanned at identical fluorescein isothiocyanate detection settings.

Chemical Analyses

Uronic acid content was determined in tissue slurry obtained by mixing the frozen tissue powder with a CDTA-containing buffer, as described above, and applying the Blumenkrantz and Asboe-Hansen method according to Kim and Carpita (1992). Pectin analyses were replicated with similar results using material grown in two independent experiments in the greenhouse. Results from one of the experiments are shown.

PME Activity Assays

PME Activity Measurement

Soluble and ionically bound (1 M NaCl-extractable) proteins were isolated from the frozen tissue powder as previously described (Micheli et al., 2000). PME activity was measured spectrophotometrically, using a Pharmacia LKB Biochrom 4060 UV-visible spectrophotometer, by monitoring pH changes resulting from de-esterification of citrus pectin (methylesterified at 89%; Sigma) with methyl red indicator (Micheli et al., 2000). The starting pH of the reaction mixture was 6.1. Readings were taken within the linear range of the reaction rate. PME activity was expressed in micromoles of H^+ released during 1 h/mg of proteins determined by DC protein assay (Bio-Rad). PME activity measurement was replicated with similar results using material grown in two independent experiments in the greenhouse. Results from one of the experiments are shown.

Isoelectric Focusing of PME

Cell wall proteins were extracted with 1 M NaCl as described above and fractionated on ultrathin polyacrylamide slab gels containing 10% (v/v) pharmalytes (pH range, 3–10; Amersham Biosciences). Before loading, samples were desalted and calibrated to 20, 100, and 200 μg of lyophilized cell wall material. Zymograms of the PMEs were generated according to Micheli et al. (2000), and the apparent pIs of the detected PMEs were determined by reference to pI markers (Bio-Rad).

Statistical Analysis

Statistical analysis of NMR data was described above. Other data were analyzed by type III ANOVA using the GLM procedure (SAS) with the following model:

$$Y = \mu + genotype + ERROR$$

If the ANOVA analysis showed a significant ($P \leq 0.05$) genotype effect, the Duncan multiple-range test was applied to test differences among genotypes at $P \leq 5\%$, or in some cases pairwise Student's t test was used to test for a difference between a transgenic line and the wild type.

Sequence data from this article can be found in the GenBank/EMBL data libraries under accession number AJ277547 (*PttPME1*).

Supplemental Data

The following materials are available in the online version of this article.

Supplemental Figure S1. Statistical analysis of NMR data.

Supplemental Table S1. *PME* genes identified in EST libraries prepared from woody tissues.

ACKNOWLEDGMENTS

We thank Dr. W.G.T. Willats and Dr. J.P. Knox for the antibodies and Mr. K. Olofsson for technical assistance.

Received October 30, 2007; accepted November 24, 2007; published December 7, 2007.

LITERATURE CITED

Alexandre F, Morvan O, Gaffe J, Mareck A, Jauneau A, Dauchel H, Balange AP, Morvan C (1997) Pectin methylesterase pattern in flax seedlings during their development. Plant Physiol Biochem **35:** 427–436

Al-Qsous S, Carpentier E, Klein-Eude D, Burel C, Mareck A, Dauchel H, Gomord V, Balange AP (2004) Identification and isolation of a pectin

methylesterase isoform that could be involved in flax cell wall stiffening. Planta **219:** 369–378

Atkinson RG, Schroder R, Hallett IC, Cohen D, MacRae EA (2002) Overexpression of polygalacturonase in transgenic apple trees leads to a range of novel phenotypes involving changes in cell adhesion. Plant Physiol **129:** 122–133

Baluška F, Hlavacka A, Šamaj J, Palme K, Robinson DG, Matoh T, McCurdy DW, Menzel D, Volkmann D (2002) F-actin-dependent endocytosis of cell wall pectins in meristematic root cells. Insights from brefeldin A-induced compartments. Plant Physiol **130:** 422–431

Berlyn GP, Miksche JP (1976) Botanical Microtechnique and Cytochemistry. Iowa State University Press, Ames, IA

Bosch M, Cheung AY, Hepler PK (2005) Pectin methylesterase, a regulator of pollen tube growth. Plant Physiol **138:** 1334–1346

Bouton S, Leboeuf E, Mouille G, Leydecker MT, Talbotec J, Granier F, Lahaye M, Hofte H, Truong HN (2002) *QUASIMODO1* encodes a putative membrane-bound glycosyltransferase required for normal pectin synthesis and cell adhesion in *Arabidopsis*. Plant Cell **14:** 2577–2590

Box GEP, Hunter WG, Hunter JS (1978) Statistics for Experimenters: An Introduction to Design, Data Analysis and Model Building. John Wiley & Sons, New York

Carpita N, McCann M (2000) The cell wall. *In* BB Buchanan, W Gruissem, RL Jones, eds, Biochemistry and Molecular Biology of Plants. American Society of Plant Physiologists, Rockville, MD, pp 52–108

Catoire L, Pierron M, Morvan C, Hervé du Penhoat C, Goldberg R (1998) Investigation of the action patterns of pectin methylesterase isoforms through kinetic analyses and NMR spectroscopy. Implications in cell wall expansion. J Biol Chem **273:** 33150–33156

Chang S, Puryear J, Cairney J (1993) A simple and efficient method for isolating RNA from pine trees. Plant Mol Biol Rep **11:** 113–116

Church G, Gilbert W (1984) Genomic sequencing. Proc Natl Acad Sci USA **81:** 1991–1995

Clausen MH, Willats WGT, Knox JP (2003) Synthetic methyl hexagalacturonate hapten inhibitors of antihomogalacturonan monoclonal antibodies LM7, JIM5 and JIM7. Carbohydr Res **338:** 1797–1800

Cosgrove DJ (2005) Growth of the plant cell wall. Nat Rev Mol Cell Biol **6:** 850–861

Di Matteo A, Giovane A, Raiola A, Camardella L, Bonivento D, De Lorenzo G, Cervone F, Bellincampi D, Tsernoglou D (2005) Structural basis for the interaction between pectin methylesterase and a specific inhibitor protein. Plant Cell **17:** 849–858

Derbyshire P, McCann MC, Roberts K (2007) Restricted cell elongation in Arabidopsis hypocotyls is associated with a reduced average pectin esterification level. BMC Plant Biol **7:** 31

Dorokhov YL, Skurat EV, Frolova OY, Gasanova TV, Ivanov PA, Ravin NV, Skryabin KG, Makinen KM, Klimyuk VI, Gleba YY, et al (2006) Role of the leader sequence in tobacco pectin methylesterase secretion. FEBS Lett **580:** 3329–3334

Doyle J, Doyle J (1989) Isolation of plant DNA from fresh tissues. Focus **12:** 13–15

Eriksson ME, Israelsson M, Olsson O, Moritz T (2000) Increased gibberellin biosynthesis in transgenic trees promotes growth, biomass production and xylem fiber length. Nat Biotechnol **18:** 784–788

Evert RF (2006) Esau's Plant Anatomy. John Wiley & Sons, Hoboken, NJ

Ezaki N, Kido N, Takahashi K, Katou K (2005) The role of wall Ca^{2+} in the regulation of wall extensibility during the acid-induced extension of soybean hypocotyl cell walls. Plant Cell Physiol **46:** 1831–1838

Fang G, Hammar S, Grumet R (1992) A quick and inexpensive method for removing polysaccharides from plant genomic DNA. Biotechniques **13:** 52–55

Femenia A, Garosi P, Roberts K, Waldron KW, Selvendran RR, Robertson JA (1998) Tissue-related changes in methyl-esterification of pectic polysaccharides in cauliflower (*Brassica oleracea* L. var. *botrytis*) stems. Planta **205:** 438–444

Francis KE, Lam SY, Copenhaver GP (2006) Separation of Arabidopsis pollen tetrads is regulated by *QUARTET1*, a pectin methylesterase gene. Plant Physiol **142:** 1004–1013

Fujino T, Itoh T (1998) Changes in pectin structure during epidermal cell elongation in pea (*Pisum sativum*) and its implications for cell wall architecture. Plant Cell Physiol **39:** 1315–1323

Geisler-Lee J, Geisler M, Coutinho PM, Segerman B, Nishikubo N, Takahashi J, Aspeborg H, Djerbi S, Master E, Andersson-Gunnerås S, et al (2006) Poplar carbohydrate-active enzymes. Gene identification and expression analyses. Plant Physiol **140:** 1–17

Goldberg R, Morvan C, Roland JC (1986) Composition, properties and localization of pectins in young and mature cells of the mung bean hypocotyl. Plant Cell Physiol **27:** 417–429

Grasdalen H, Bakoy OE, Larsen B (1988) Determination of the degree of esterification and the distribution of methylated and free carboxyl groups in pectins by h-1-nmr spectroscopy. Carbohydr Res **184:** 183–191

Gray-Mitsumune M, Mellerowicz EJ, Abe H, McQueen-Mason S, Winzéll A, Sterky F, Blomqvist K, Schrader J, Teeri TT, Sundberg B (2004) Expansins abundant in secondary xylem belong to subgroup a of the α-expansin gene family. Plant Physiol **135:** 1552–1564

Gray-Mitsumune M, Blomquist K, McQueen-Mason S, Teeri TT, Sundberg B, Mellerowicz EJ (2007) Ectopic expression of a wood-abundant expansin *PttEXPA1* promotes cell expansion in primary and secondary tissues in aspen. Plant Biotechnol J **6:** 62–72

Guglielmino N, Liberman M, Catesson AM, Mareck A, Prat R, Mutaftschiev S, Goldberg R (1997a) Pectin methylesterases from poplar cambium and inner bark: localization, properties and seasonal changes. Planta **202:** 70–75

Guglielmino N, Liberman M, Jauneau A, Vian B, Catesson AM, Goldberg R (1997b) Pectin immunolocalization and calcium visualization in differentiating derivatives from poplar cambium. Protoplasma **199:** 151–160

Hasunuma T, Fukusaki E, Kobayashi A (2004) Expression of fungal pectin methylesterase in transgenic tobacco leads to alteration in cell wall metabolism and a dwarf phenotype. J Biotechnol **111:** 241–251

Israelsson M, Eriksson ME, Hertzberg M, Aspeborg H, Nilsson P, Moritz T (2003) Changes in gene expression in the wood-forming tissue of transgenic hybrid aspen with increased secondary growth. Plant Mol Biol **52:** 893–903

Iwai H, Ishii T, Satoh S (2001) Absence of arabinan in the side chains of the pectic polysaccharides strongly associated with cell walls of *Nicotiana plumbaginifolia* non-organogenic callus with loosely attached constituent cells. Planta **213:** 907–915

Iwai H, Masaoka N, Ishii T, Satoh S (2002) A pectin glucuronyltransferase gene is essential for intercellular attachment in the plant meristem. Proc Natl Acad Sci USA **99:** 16319–16324

Jarvis MC (1984) Structure and properties of pectin gels in plant cell walls. Plant Cell Environ **7:** 153–164

Jarvis MC, Briggs SPH, Knox JP (2003) Intercellular adhesion and cell separation in plants. Plant Cell Environ **26:** 977–989

Jiang LX, Yang SL, Xie LF, Puah CS, Zhang XQ, Yang WC, Sundaresan V, Ye D (2005) VANGUARD1 encodes a pectin methylesterase that enhances pollen tube growth in the *Arabidopsis* style and transmitting tract. Plant Cell **17:** 584–596

Kay LE, Keifer P, Saarinen T (1992) Pure absorption gradient enhanced heteronuclear single quantum correlation spectroscopy with improved sensitivity. J Am Chem Soc **114:** 10663–10665

Kim JB, Carpita NC (1992) Changes in esterification of the uronic acid groups of cell wall polysaccharides during elongation of maize coleoptiles. Plant Physiol **98:** 646–653

Koncz C, Schell J (1986) The promoter of T_L-DNA gene 5 controls the tissue-specific expression of chimaeric genes carried by a novel type of *Agrobacterium* binary vector. Mol Gen Genet **204:** 383–396

Lacoux J, Klein D, Domon JM, Burel C, Lamblin F, Alexandre F, Sihachakr D, Roger D, Balange AP, David A, et al (2003) Antisense transgenesis of *Linum usitatissimum* with a pectin methylesterase cDNA. Plant Physiol Biochem **41:** 241–249

Lamblin F, Saladin G, Dehorter B, Cronier D, Grenier E, Lacoux J, Bruyant P, Laine E, Chabbert B, Girault F, et al (2001) Overexpression of a heterologous *sam* gene encoding S-adenosylmethionine synthetase in flax (*Linum usitatissimum*) cells: consequences on methylation of lignin precursors and pectins. Physiol Plant **112:** 223–232

Larson PR (1994) The Vascular Cambium. Springer-Verlag, Berlin

Leboeuf E, Guillon F, Thoiron S, Lahaye M (2005) Biochemical and immunohistochemical analysis of pectic polysaccharides in the cell walls of Arabidopsis mutant *QUASIMODO 1* suspension-cultured cells: implications for cell adhesion. J Exp Bot **56:** 3171–3182

Lev-Yadun S (2001) Intrusive growth—the plant analog of dendrite and axon growth in animals. New Phytol **150:** 508–512

Limberg G, Korner R, Buchholt HC, Christensen TMIE, Roepstorff P, Mikkelsen JD (2000) Analysis of pectin structure part 1—analysis of

different de-esterification mechanisms for pectin by enzymatic fingerprinting using endopectin lyase and endopolygalacturonase II from *A. niger.* Carbohydr Res **327:** 293–307

Liners F, Gaspar T, Vancutsem P (1994) Acetyl-esterification and methyl-esterification of pectins of friable and compact sugar-beet calli—consequences for intercellular-adhesion. Planta **192:** 545–556

Louvet R, Cavel E, Gutierrez L, Guenin S, Roger D, Gillet F, Guerineau F, Pelloux J (2006) Comprehensive expression profiling of the pectin methylesterase gene family during silique development in *Arabidopsis thaliana.* Planta **224:** 782–791

Mellerowicz EJ, Baucher M, Sundberg B, Bojeran W (2001) Unravelling cell wall formation in the woody dicot stem. Plant Mol Biol **47:** 239–274

Micheli F (2001) Pectin methylesterases: cell wall enzymes with important roles in plant physiology. Trends Plant Sci **6:** 414–419

Micheli F, Holliger C, Goldberg R, Richard L (1998) Characterization of the pectin methylesterase-like gene *AtPME3*: a new member of a gene family comprising at least 12 genes in *Arabidopsis thaliana*. Gene **220:** 13–20

Micheli F, Sundberg B, Goldberg R, Richard L (2000) Radial distribution pattern of pectin methylesterases across the cambial region of hybrid aspen at activity and dormancy. Plant Physiol **124:** 191–199

Orfila C, Huisman MMH, Willats WGT, van Alebeek GJWM, Schols HA, Seymour GB, Knox JP (2001) Altered middle lamella homogalacturonan and disrupted deposition of (1→5)-α-L-arabinan in the pericarp of *cnr*, a ripening mutant of tomato. Plant Physiol **126:** 210–221

Parre E, Geitmann A (2005) Pectin and the role of the physical properties of the cell wall in pollen tube growth of *Solanum chacoense.* Planta **220:** 582–592

Pelloux J, Rustérucci C, Mellerowicz EJ (2007) New insights into pectin methylesterase structure and function. Trends Plant Sci **12:** 267–277

Pilling J, Willmitzer L, Bückimg H, Fishan J (2004) Inhibition of a ubiquitously expressed pectin methyl esterase in *Solanum tuberosum* L. affects plant growth, leaf growth polarity, and ion partitioning. Planta **219:** 32–40

Pilling J, Willmitzer L, Fisahn J (2000) Expression of a *Petunia inflata* pectin methyl esterase in *Solanum tuberosum* L. enhances stem elongation and modifies cation distribution. Planta **210:** 391–399

Proseus TE, Boyer JS (2006) Calcium pectate chemistry controls growth rate of Chara corallina. J Exp Bot **57:** 3989–4002

Rhee SY, Somerville CR (1998) Tetrad pollen formation in quartet mutants of *Arabidopsis thaliana* is associated with persistence of pectic polysaccharides of the pollen mother cell wall. Plant J **15:** 79–88

Romberger JA (1963) Meristems, Growth and Development in Woody Plants. Technical Bulletin No. 1293. Forest Service, U.S. Department of Agriculture, Washington, DC

Rosenbohm C, Lundt I, Christensen TMIE, Young NWG (2003) Chemically methylated and reduced pectins: preparation, characterisation by ^{1}H NMR spectroscopy, enzymatic degradation, and gelling properties. Carbohydr Res **338:** 637–649

Schrader J, Nilsson J, Mellerowicz E, Berglund A, Nilsson P, Hertzberg M, Sandberg G (2004) A high-resolution transcript profile across the wood-forming meristem of poplar identifies potential regulators of cambial stem cell identity. Plant Cell **16:** 2278–2292

Shani Z, Dekel M, Tsabary G, Goren R, Shoseyov O (2004) Growth enhancement of transgenic poplar plants by overexpression of Arabidopsis thaliana endo-1,4-0-glucanase (cel1). Mol Breed **14:** 321–330

Shani Z, Dekel M, Tsabary G, Jensen CS, Tzfira T, Goren R, Altman A, Shoseyov O (1999) Expression of *Arabidopsis thaliana*, endo-1,4-β-glucanase (*cel*1) in transgenic poplar plants. *In* A Altman, M Ziv, S Izhar, eds, Plant Biotechnology and In Vitro Biology in the 21st Century. Kluwer Academic Publishers, Dordrecht, The Netherlands, pp 209–212

Shi HZ, Kim Y, Guo Y, Stevenson B, Zhu JK (2003) The Arabidopsis SOS5 locus encodes a putative cell surface adhesion protein and is required for normal cell expansion. Plant Cell **15:** 19–32

Singh SK, Eland C, Harholt J, Scheller HV, Marchant A (2005) Cell adhesion in Arabidopsis thaliana is mediated by ECTOPICALLY PARTING CELLS 1—a glycosyltransferase (GT64) related to the animal exostosins. Plant J **43:** 384–397

Sterky F, Regan S, Karlsson J, Hertzberg M, Rohde A, Holmberg A, Amini B, Bhalerao R, Larsson M, Villarroel R, et al (1998) Gene discovery in the wood-forming tissues of poplar: analysis of 5692 expressed sequence tags. Proc Natl Acad Sci USA **95:** 13330–13335

Takahata K, Takeuchi M, Fujita M, Azuma J, Kamada H, Sato F (2004) Isolation of putative glycoprotein gene from early somatic embryo of carrot and its possible involvement in somatic embryo development. Plant Cell Physiol **45:** 1658–1668

Tieman DM, Harriman RW, Ramamohan G, Handa AK (1992) An antisense pectin methylesterase gene alters pectin chemistry and soluble solids in tomato fruit. Plant Cell **4:** 667–679

van Alebeek GJWM, Christensen TMIE, Schols HA, Mikkelsen JD, Voragen AGJ (2002) Mode of action of pectin lyase A of *Aspergillus niger* on differently C-6-substituted oligogalacturonides. J Biol Chem **277:** 25929–25936

von Heijne G (1986) A new method for predicting signal sequence cleavage sites. Nucleic Acids Res **14:** 4683–4690

Wehr JB, Menzies NW, Blamey FPC (2004) Inhibition of cell-wall autolysis and pectin degradation by cations. Plant Physiol Biochem **42:** 485–492

Wen F, Zhu Y, Hawes MC (1999) Effect of pectin methylesterase gene expression on pea root development. Plant Cell **11:** 1129–1140

Wenham MW, Cusick F (1975) The growth of secondary fibres. New Phytol **74:** 247–261

Willats WGT, Knox JP (1999) Immunoprofiling of pectic polysaccharides. Anal Biochem **268:** 143–146

Willats WGT, Limberg G, Buchholt HC, van Alebeek GJ, Benen J, Christensen TMIE, Visser J, Voragen A, Mikkelsen JD, Knox JP (2000) Analysis of pectin structure part 2—analysis of pectic epitopes recognised by hybridoma and phage display monoclonal antibodies using defined oligosaccharides, polysaccharides, and enzymatic degradation. Carbohydr Res **327:** 309–320

Willats WGT, Orfila C, Limberg G, Buchholt HC, van Alebeek GJWM, Voragen AGJ, Marcus SE, Christensen TMIE, Mikkelsen JD, Murray BS, et al (2001) Modulation of the degree and pattern of methyl-esterification of pectic homogalacturonan in plant cell walls. J Biol Chem **276:** 19404–19413

Zhang GF, Staehelin LA (1992) Functional compartmentation of the Golgi apparatus of plant cells. Immunocytochemical analysis of high-pressure frozen- and freeze-substituted sycamore maple suspension culture cells. Plant Physiol **99:** 1070–1083